Dopant-modulated conjugated polymer enrichment of semiconducting SWCNTs

Li, Zhao; Ding, Jianfu; Lefebvre, Jacques; Malenfant, Patrick R. L.

Publisher's version / Version de l'éditeur:
https://doi.org/10.1021/acsomega.8b00383
ACS Omega, 3, 3, pp. 3413-3419, 2018-03-21

ACS OMEGA

Article

Cite This: ACS Omega 2018, 3, 3413−3419

Dopant-Modulated Conjugated Polymer Enrichment of Semiconducting SWCNTs

Zhao Li,* Jianfu Ding, Jacques Lefebvre, and Patrick R. L. Malenfant*

Security and Disruptive Technologies Portfolio, National Research Council Canada, 1200 Montreal Road, Ottawa, Ontario K1A 0R6, Canada

Supporting Information

ABSTRACT: Conjugated polymer extraction (CPE) is a low-cost, scalable process that can enrich single-walled carbon nanotube (SWCNT) materials in organic media. For other separation methods in aqueous phases, redox chemistry and/or pH control dramatically affect the sorting process of the SWCNTs. We have previously determined that the CPE process can be fine-tuned by adjusting the pH on the tube surface. Here, we systematically studied the effect of redox chemistry on the CPE process by adding organic p-/n-dopants. At a very strong p-/n-doping level, static repulsions dominated the interactions between the tubes and the CPE lost selectivity. When the doping level changed from a medium p-doping to a neutral state, the yield of CPE increased and the selectivity was compromised. We also observed chiral selectivity when a weak p-dopant was used. A photoluminescence excitation mapping under different titration conditions provided more insight into the doping level of the tubes relative to their diameters, chiralities, and redox potentials. We proposed a mechanism for the CPE process. The semiconducting and metallic tubes are separated because of their different solubilities, which are determined by the bundling energy between the tubes and are related to their doping level in polymer solutions.

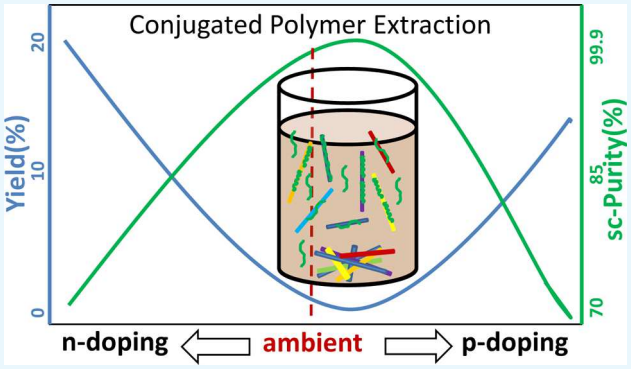

1. INTRODUCTION

Recently, conjugated polymer extraction (CPE) has been extensively studied for the enrichment of single-walled carbon nanotubes (SWCNTs).[1−4] Compared with other sorting methods, such as density gradient ultracentrifugation, gel chromatography, and the recently developed two-phase extraction, the CPE process has several obvious advantages.[1−6] First, its cost is very low. Only a regular bath or tip sonication and a low-speed centrifuge are required for instrumentation. The cost of the polymer can also be reduced if polymers with simple structures, such as polythiophene or polyfluorene, are used. Moreover, this cost can be further dramatically reduced if recyclable polymers are used.[7] Second, this process is scalable, and it is only restricted by the capacities of the sonicator and the centrifuge, which can be improved with a continuous flow-through apparatus. Third, the obtained products have a high concentration and tube content due to the strong interaction of the polymers with the tubes and the high affinity of the organic solvents for the tubes. In practice, in a stable tube/polymer dispersion, the tube/polymer weight ratio can reach 1/1 and the tube concentration can be more than 0.5 g/L. Both values are much higher than those obtained via an aqueous process. Fourth, the semiconducting (sc) purity of the CPE product can be greater than 99.9%, which is sufficient for some low-end applications.[8] In addition, the nature of the organic phase can add other benefits to the application of these materials. For example, we found that these organic phase dispersions can be easily deposited on substrates to form high-density networks and high-performance thin film transistors can be easily fabricated.[9]

Until now, most of the work in this field has focused on investigating different polymer structures.[1−6,10,11] Although some of these experiments are quite successful, the control of the yield and the selectivity are still challenging, and the selection mechanism is not well understood. Recently, Cuniberti et al. proposed that the diameter selectivity mechanism is a competition between tube bundling and polymer adsorption.[12] Their simulation agrees well with other experimental findings regarding the diameter selectivity, but this mechanism failed to explain the more important electric-type selectivity of the sorting process and the nature of the bundling between the different types of tubes.

The redox chemistry and pH affect the sorting of SWCNTs in aqueous systems.[13−16] Zheng et al. found that redox molecules trigger the reorganization of the surfactant coating layer on SWCNTs in aqueous two-phase systems.[17] In addition, they noted that the solubility of polymer-wrapped SWCNTs in organic solvents strongly depends on the redox status. Recently,

Received: March 2, 2018
Accepted: March 12, 2018
Published: March 21, 2018

Scheme 1. Structures of the Dopants Used in This Study

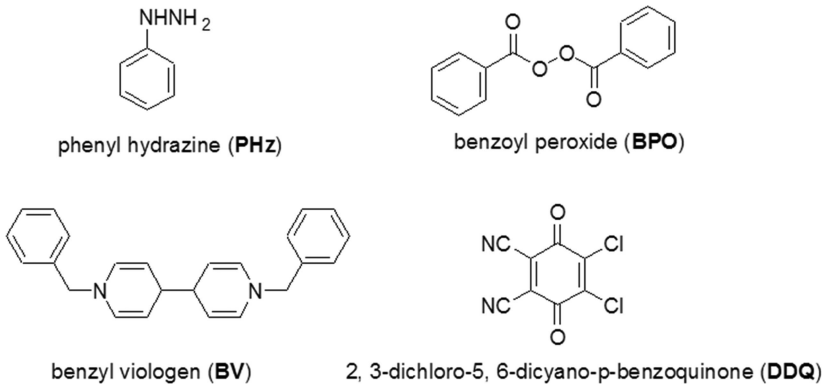

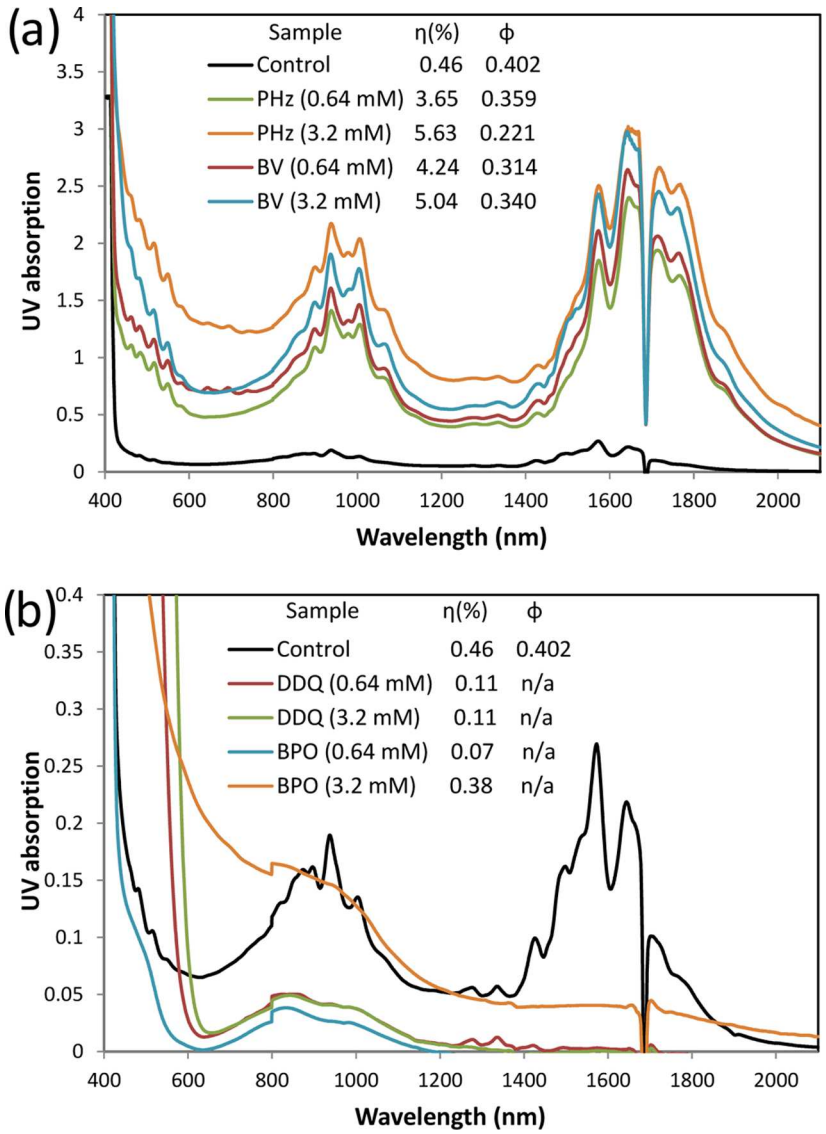

Figure 1. Representative absorption spectra of the supernatants from the second PFDD extraction of the SWCNT samples with the addition of (a) n-type and (b) p-type dopants. The inset shows the yield (η%) and ϕ value.

our group reported that adjusting the surface acidity of SWCNTs via the addition of sodium hydroxide dramatically influences the CPE process.[18] The selective mechanism for the dispersion of semiconducting versus metallic (m) carbon nanotube (CNT) was attributed to oxygen doping under ambient conditions, which will preferentially cause the bundling of highly polarizable metallic (m) tubes.

In this article, we further expanded the range of the redox doping level using organic dopants in addition to oxygen/water redox couples to investigate their effect on the CPE of

DOI: 10.1021/acsomega.8b00383
ACS Omega 2018, 3, 3413−3419

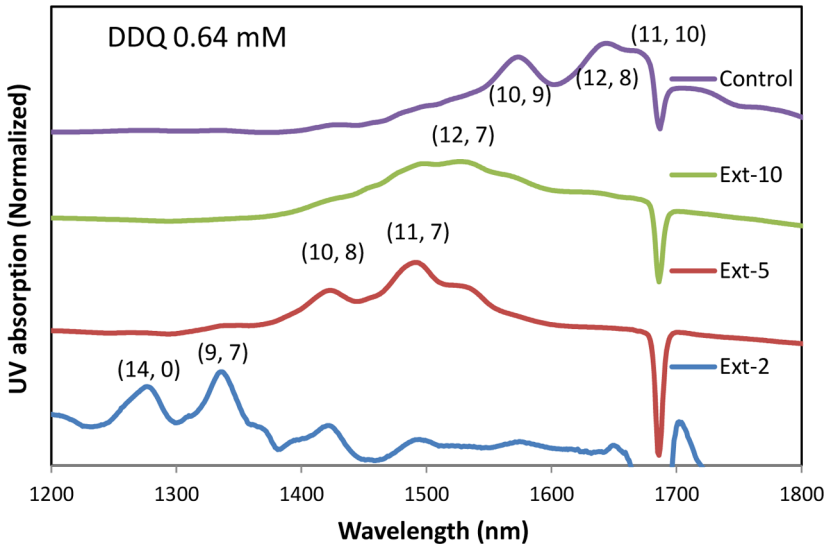

Figure 2. Absorption spectra of the supernatants from the PFDD extractions of SWCNTs in the presence of 0.64 mM DDQ. Only spectra from 2nd, 5th, and 10th extractions are shown, and the spectra are normalized and stacked. Control spectrum is from second extraction without addition of any dopants.

SWCNTs. We found that both the yield and purity of the SWCNTs from the CPE of raw tube materials can be modulated by the dopants. We also observed chirality selectivity under certain doping conditions, which was related to the energy level and/or diameter of the tubes. The photoluminescence excitation (PLE) mapping titration study of the tube solutions under different doping levels further revealed the mechanism of this diameter selectivity. This new insight provides guiding principles in sc-SWCNT enrichment, allowing further control on both the chirality and semiconducting purity of a key enabling material in high-end and printed electronics.[19]

2. RESULTS AND DISCUSSION

The structures of the four dopants are shown in Scheme 1.[20] They all contain benzene rings in their structures, which can improve both their solubility in toluene and affinity for SWCNTs.[21−24] SWCNTs can be amphoterically doped via encapsulation of organic molecules within the SWCNTs, and the charge transfer is controlled via the ionization potential or electron affinity of the guest molecules.[25,26] For plasma torch-synthesized, raw SWCNTs with an average diameter of 1.3 nm, phenyl hydrazine (PHz) and benzyl viologen (BV) donate electrons (n-doping) to and benzoyl peroxide (BPO) and 2,3-dichloro-5,6-dicyano-*p*-benzoquinone (DDQ) withdraw electrons (p-doping) from the tubes depending on the redox potential of the dopants.[27] We added a certain amount of the dopants into a poly(9,9-di-*n*-docecylfluorene) (PFDD) solution, and CPEs were performed under the same conditions.[28] The detailed experimental procedure and spectra can be found in the Supporting Information (SI) (Figures S1−S5).

In summary, the UV absorption spectra, yield, and ϕ value from the supernatant of the second extraction are shown in Figure 1.[28] We chose the second extraction as typical data because we found that the first extraction heavily depends on source materials and their pretreatment, which determines the initial doping state of the materials and will affect the CPE process as will be demonstrated in this work. Here, ϕ is the ratio of the integrated areas of only the S_{22} band to that of the S_{22} band plus its background, which can be closely related to the purity level and ranges from 0.07 to 0.42 corresponding from raw materials to high-sc-purity samples.[4] The *y* axis (UV absorption) was not normalized, and the peak intensity can be directly related to the tube concentration and yield. Clearly, the addition of PHz or BV dramatically improves the yield of the CPE process. In a regular control experiment, the yield for the first extraction is usually less than 0.3% and the total yield for the first four extractions is 3.39%. A higher yield of 2.82% appears in the fifth extraction. However, when a very small amount of PHz or BV (0.64 mM or 2.1% relative to the carbon in the raw material) is added, the yields of the first and second extractions are over 1 and 4%, respectively, and the yield of the first four extractions improves to over 10%. The sc-purity only slightly decreases to a ϕ value of ∼0.33, corresponding to 99% pure sc-SWCNTs.[8] The addition of a higher concentration of n-dopants further slightly increases the yield, but the purity is compromised. The yield and purity of the CPE can also be adjusted by changing the polymer/tube ratio or solution concentration, but these methods are less effective.[28]

Interestingly, the addition of 0.64 mM p-dopant (DDQ or BPO) leads to a very low yield (∼0.1%). A further addition of BPO (3.2 mM) improves the yield to 0.38% but at the cost of the selectivity. The quenching of the bands at S_{11} (1200−1900 nm) is due to the increased p-doping level, whereas the bands at S_{22} (700−1100) are not severely affected by the addition of these dopants (Figure S6).[20,29] Two small peaks at 1275 and 1335 nm emerge in the spectrum of the second extraction when 0.64 mM DDQ is added. We performed additional CPE on this precipitate, and the normalized spectra are shown in Figure 2. Clearly, this CPE shows chirality selectivity, and the small-diameter tubes ((14, 0) or (9, 7)) are extracted first, followed by the middle-diameter tubes ((10, 8) and (11, 7)) and the large-diameter tubes ((10, 9), (12, 8), and (11, 10)). In the Raman spectra of the filtered solid sample from these fractions (Figure S7 in SI), the radial breathing mode (RBM) bands clearly confirm that the smaller-diameter tubes are extracted out first because the RBM frequency of the Raman shift is the reciprocal of the diameter of the tubes.[30] Zheng et al. also observed similar chirality selectivity in their redox sorting of SWCNTs in an aqueous phase.[17]

DOI: 10.1021/acsomega.8b00383
ACS Omega 2018, 3, 3413−3419

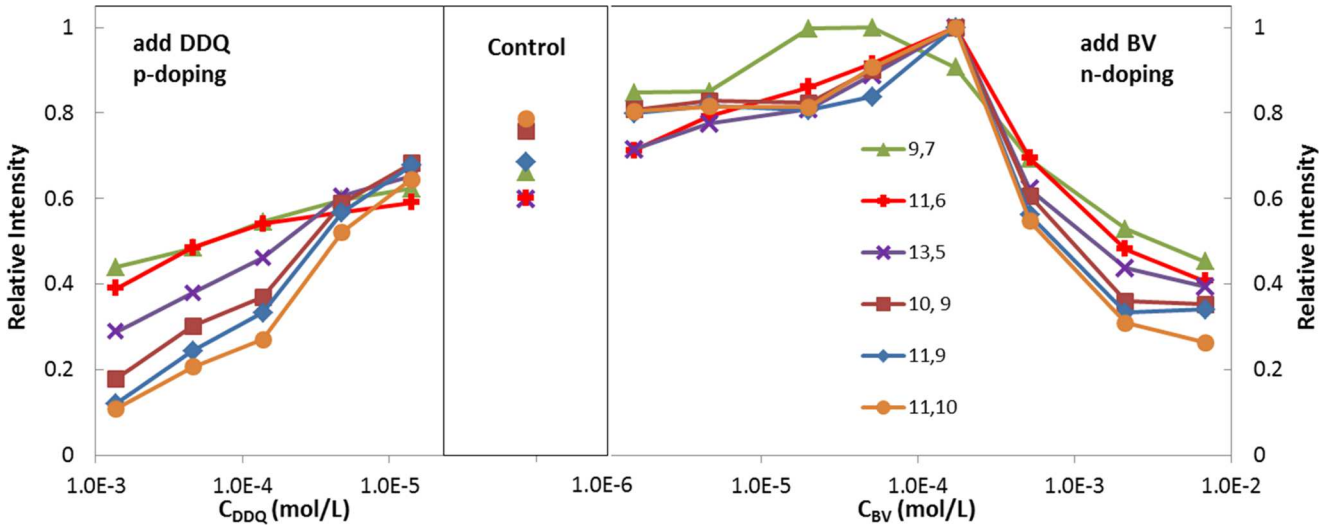

Figure 3. Relative fluorescence intensity of six sc-SWCNT (C_{CNT} = 8.0 mg/L) species in a PFDD (C_{PFDD} = 34.7 mg/L) toluene solution with the addition of the p-dopant DDQ (left) or n-dopant BV (right).

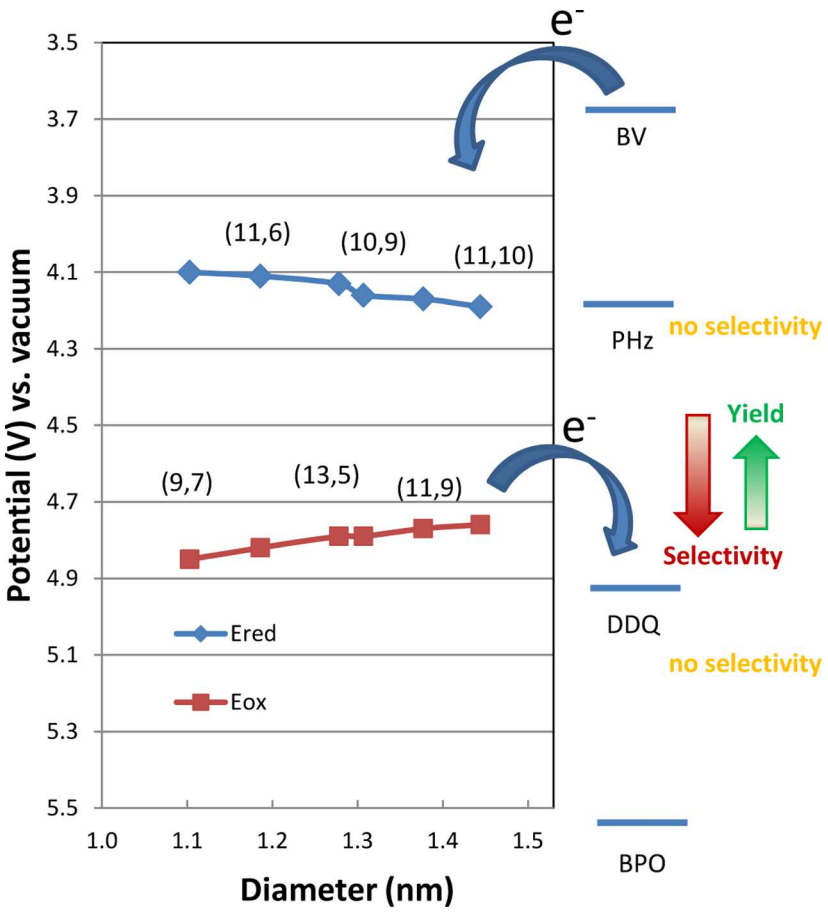

Figure 4. Reduction and oxidation potentials of the (n, m) SWCNTs as a function of the nanotube diameter.[41] The energy levels of the four dopants used in this study are also shown. The right side scheme shows the relationship between the selectivity and yield of the CPE process with the SWCNT samples and the Fermi level of the system.

To further explore the effects of the dopants on the CPE of SWCNTs, PLE maps were tracked in a series of titration experiments in a high-purity sc-SWCNT/PFDD solution, and the spectra are shown in Figures S8 and S9 of the SI.[31] We monitored the fluorescence intensity of six (n, m) species (labeled on Figure S8A and listed in Table S1), and the relationship of the relative intensity and the dopant concentration is drawn in Figure 3.[32,33] Under ambient conditions, SWCNTs are slightly p-doped because of the H_2O/O_2 redox couple.[34−38] Therefore, the addition of the n-dopant BV first neutralizes this p-doping effect, resulting in a corresponding increase in the fluorescence intensity.[20,39] This

DOI: 10.1021/acsomega.8b00383
ACS Omega 2018, 3, 3413−3419

effect reaches a plateau when the concentration of BV is approximately 1.75×10^{-4} mol/L and the ratio of the BV/C atoms in the tubes is 1/3.8. Then, the sc-tubes reach an electrically neutral state, and the valence band is fully filled, whereas the conduction band is still empty. Further addition of BV leads to a rapid decrease in the fluorescence intensity because of n-doping, and the conduction band is partially filled by electrons. The addition of the p-dopant DDQ to the control sample reduces the fluorescence intensity of the tubes because of the enhanced p-doping level.[20] More importantly, the decrease in the fluorescence intensity of the larger-diameter tubes is faster than that of the small-diameter tubes at the same dopant concentration, and this difference was further demonstrated by their energy levels, which we will discuss in the following section. Doorn et al. also reported a similar chiral-selective bleaching of SWCNTs in an aqueous phase with organic acceptor molecules.[40]

Next, the CPE mechanism for SWCNTs with different redox states was considered.[17] The redox potentials of six representative sc-tubes and dopants are plotted in Figure 4.[23,41,42] Under very high p-/n-doped conditions, all of the m/sc-tubes are highly positively or negatively charged and the electrostatic repulsion between the tubes dominates their interaction. Because of this, selective bundling of the tubes does not occur and the CPE loses its selectivity. The reported spontaneous dissolution of reduced nanotubes by metal anions in polar aprotic solvents can be ascribed to the high n-doping.[43−45] Smalley et al. also reported the high solubility of SWCNTs in superacids via direct protonation, which is in the highly p-doped region.[46]

Under ambient conditions, the tubes are slightly p-doped because of the H_2O/O_2 redox couple, and their doping level can be easily adjusted with the addition of p-/n-dopants.[20,35−37] Upon addition of n-dopants (BV or PHz), the yield improves at the cost of the selectivity, corresponding to the gradual removal of the slightly p-doped state. This trend continues until the tubes reach a neutral state, and then, the CPE completely loses selectivity.[35] The effect of PHz is more obvious because it is an n-dopant and an efficient oxygen scavenger.[42] In contrast, after the addition of p-dopants, the CPE has a poor yield but chiral selectivity can be obtained under certain conditions. The oxidation potential of DDQ is closer to that of the sc-tubes. The addition of a small amount of DDQ selectively p-dopes the larger-diameter tubes, and the small-diameter tubes are extracted first, which agrees well with the photoluminescence titration results.[35,47,48] Although BPO is a stronger p-dopant than DDQ because of its oxidation potential, it dopes all of the sc-tubes, and no chiral selectivity is observed during the CPE.[49]

Clearly, the yield and selectivity can be effectively adjusted by adding dopants in the middle region, as shown in Figure 4, where the Fermi level of the system is located between 4.47 eV (neutral state for the SWCNTs) and ∼5.0 eV (medium p-doping). Fortunately, the CPE under ambient conditions is located within the desired region with a high selectivity and median yield. Interestingly, in 0.64 mM BPO, the total yield of the first four extractions is only 0.4%, which means that almost all of the tubes form bundles and precipitate out at this doping level. These results demonstrate that the p-doping level of the sc-tubes determines their bundling tendency and solubility in the PFDD/toluene solution. For the m-tubes, the change in their electrical properties is less pronounced within this range because of their continuous electric density of state.[20,23]

We propose that the separation mechanism of the CPE process can be rationalized by considering the electric properties and polarizability of the m/sc-tubes.[50,51] The doping level is determined by both the redox potential of the dopants and their concentration, and it may also be related to the thermal distribution of the electrons.[52] In the highly n/p-doped state, electrostatic repulsions dominate and both the m/sc-tubes are extracted without any selectivity. In the medium p-doped to neutral state range, the m-tubes have a very low solubility and the solubility of the sc-tubes is related to their p-doping level, which is determined by their diameters/chiralities and the redox potential and the concentration of the dopants. With an adequate p-doping level, the sc-tubes have enough positive charge to preferentially induce polar−polar interactions with the m-tubes, which have a 10^3−10^5 times larger polarizability, leading to selective bundling and sc-SWCNT enrichment.[53,54] Previously, we reported that m-tubes show a stronger affinity to a polar silica gel surface, which agrees with the observation here.[55] The bundling energy between the tubes is very sensitive to their doping level and careful consideration of the doping level can provide better control of the electrical-type and/or diameter selectivity.[38]

In these experiments, PFDD acts like a neutral polymer and charge transfers are not observed between it and carbon nanotubes. We propose that control of the bundling/energy level is more important than polymer adsorption in a CPE process in this case.[18,56−58] However, for other polymers that contain electron-donating or -withdrawing groups or charges, the charge transfer must be considered in their interactions with the tubes.[59,60] This type of interaction is similar to that observed for the dopants and dramatically influences the CPE process, as recently reported by Adronov et al.[61] To further test the doping effect on the CPE of other polymers/SWCNTs systems, we used PFDD on CoMoCAT and P3DDT on HiPCO samples. The representative absorption curves are shown in Figure S10 (Supporting Information). Clearly, addition of p-/n-dopants will dramatically influence both the yield and chirality of SWCNT/polymer dispersions in the obtained supernatants. Several key parameters have to be considered here: diameters and initial doping states of raw SWCNT materials, polymer structures that define their interaction with SWCNTs, and the energy level of the whole system, which can be affected by addition of p-/n-dopants.

3. CONCLUSIONS

In conclusion, we studied the effects of dopants on the enrichment of SWCNT materials using a CPE process. At very high p-/n-doping levels, the static repulsions between the highly charged tubes dominate their interactions and the CPE process loses its selectivity. In the medium p-doping to neutral range, the CPE process can be efficiently modulated via the addition of n/p-dopants with a balance between the yield and the sc-purity. The dispersibility of the tubes is determined by their bundling energy, which can be further explained by their doping level. The differentiation of the sc/m-tubes comes from their electric properties and polarizabilities. We believe that this redox-modulated sorting can also work for other types of SWCNTs and polymer systems because it is sensitive only to the tube redox potentials and the bundling tendency between the tubes. This input enhances our understanding of the CPE mechanism and benefits the commercial production of SWCNT materials by allowing for better control of the yield or chirality.

DOI: 10.1021/acsomega.8b00383
ACS Omega 2018, 3, 3413−3419

■ ASSOCIATED CONTENT

Supporting Information

The Supporting Information is available free of charge on the ACS Publications website at DOI: 10.1021/acsomega.8b00383.

Materials source; typical enrichment process; characterization methods; absorption spectra of the supernatants from four successive PFDD extractions of an SWCNT sample (Figure S1), in the presence of BV (Figure S2), PHz (Figure S3), BPO (Figure S4), and DDQ (Figure S5); absorption spectra of the SWCNT/PFDD solution with the addition of dopants (Figure S6); Raman spectra of some extractions (Figure S7); PLE mapping of SWCNT/PFDD dispersion with the addition of DDQ (Figure S8) and BV (Figure S9); absorption spectra of extractions of PFDD for CoMoCAT and P3DDT for HiPCO in the presence of dopants (Figure S10); excitation and emission wavelengths of six chirality tubes (Table S1) (PDF)

■ AUTHOR INFORMATION

Corresponding Authors

*E-mail: Zhao.li@nrc.ca (Z.L.).

*E-mail: Patrick.Malenfant@nrc.ca (P.R.L.M.).

ORCID

Patrick R. L. Malenfant: 0000-0001-5391-2300

Notes

The authors declare no competing financial interest.

■ REFERENCES

(1) Wang, H.; Bao, Z. Conjugated polymer sorting of semiconducting carbon nanotubes and their electronic applications. *Nano Today* **2015**, *10*, 737−758.

(2) Fujigaya, T.; Nakashima, N. Non-covalent polymer wrapping of carbon nanotubes and the role of wrapped polymers as functional dispersants. *Sci. Technol. Adv. Mater.* **2015**, *16*, No. 024802.

(3) Samanta, S. K.; Fritsch, M.; Scherf, U.; Gomulya, W.; Bisri, S. Z.; Loi, M. A. Conjugated polymer-assisted dispersion of single-wall carbon nanotubes: the power of polymer wrapping. *Acc. Chem. Res.* **2014**, *47*, 2446−2456.

(4) Lefebvre, J.; Ding, J.; Li, Z.; Finnie, P.; Lopinski, G.; Malenfant, P. R. L. High-purity semiconducting single-walled carbon nanotubes: a key enabling material in emerging electronics. *Acc. Chem. Res.* **2017**, *50*, 2479−2486.

(5) Lei, T.; Pochorovski, I.; Bao, Z. Separation of semiconducting carbon nanotubes for flexible and stretchable electronics using polymer removable method. *Acc. Chem. Res.* **2017**, *50*, 1096−1104.

(6) Adronov, A.; Fong, D. Recent developments in the selective dispersion of single-walled carbon nanotubes using conjugated polymers. *Chem. Sci.* **2017**, *8*, 7292−7305.

(7) Lei, T.; Chen, X.; Pitner, G.; Wong, H. S. P.; Bao, Z. Removable and recyclable conjugated polymers for highly selective and high-yield dispersion and release of low-cost carbon nanotubes. *J. Am. Chem. Soc.* **2016**, *138*, 802−805.

(8) Li, Z.; Ding, J.; Finnie, P.; Lefebvre, J.; Cheng, F.; Kingston, C. T.; Malenfant, P. R. L. Raman microscopy mapping for the purity assessment of chirality enriched carbon nanotube networks in thin-film transistors. *Nano Res.* **2015**, *8*, 2179−2187.

(9) Li, Z.; Ding, J.; Lefebvre, J.; Malenfant, P. R. L. Surface effects on network formation of conjugated polymer wrapped semiconducting single walled carbon nanotubes and thin film transistor performance. *Org. Electron.* **2015**, *26*, 15−19.

(10) Jakubka, F.; Schießl, S. P.; Martin, S.; Englert, J. M.; Hauke, F.; Hirsch, A.; Zaumseil, J. Effect of polymer molecular weight and solution parameters on selective dispersion of single-walled carbon nanotubes. *ACS Macro Lett.* **2012**, *1*, 815−819.

(11) Gerstel, P.; Klumpp, S.; Hennrich, F.; Poschlad, A.; Meded, V.; Blasco, E.; Wenzel, W.; Kappes, M. M.; Barner-Kowollik, C. Highly selective dispersion of single-walled carbon nanotubes via polymer wrapping: a combinatorial study via modular conjugation. *ACS Macro Lett.* **2014**, *3*, 10−15.

(12) Yang, H.; Bezugly, V.; Kunstmann, J.; Filoramo, A.; Cuniberti, G. Diameter-selective dispersion of carbon nanotubes via polymers: a competition between adsorption and bundling. *ACS Nano* **2015**, *9*, 9012−9019.

(13) Ju, S. Y.; Utz, M.; Papadimitrakopoulos, F. Enrichment mechanism of semiconducting single-walled carbon nanotubes by surfactant amines. *J. Am. Chem. Soc.* **2009**, *131*, 6775−6784.

(14) Wang, J.; Nguyen, T. D.; Cao, Q.; Wang, Y.; Tan, M. Y. C.; Chan-Park, M. B. Selective surface charge sign reversal on metallic carbon nanotubes for facile ultrahigh purity nanotube sorting. *ACS Nano* **2016**, *10*, 3222−3232.

(15) Hirano, A.; Tanaka, T.; Urabe, Y.; Kataura, H. pH- and solute-dependent adsorption of single-wall carbon nanotubes onto hydrogels: mechanistic insights into the metal/semiconductor Separation. *ACS Nano* **2013**, *7*, 10285−10295.

(16) Ichinose, Y.; Eda, J.; Yomogida, Y.; Liu, Z.; Yanagi, K. Extraction of high-purity single-chirality single-walled carbon nanotubes through precise pH control using carbon dioxide bubbling. *J. Phys. Chem. C* **2017**, *121*, 13391−13395.

(17) Gui, H.; Streit, J. K.; Fagan, J. A.; Walker, A. R. H.; Zhou, C.; Zheng, M. Redox sorting of carbon nanotubes. *Nano Lett.* **2015**, *15*, 1642−1646.

(18) Ding, J.; Li, Z.; Lefebvre, J.; Du, X.; Malenfant, P. R. L. Mechanistic consideration of pH effect on the enrichment of semiconducting SWCNTs by conjugated polymer extraction. *J. Phys. Chem. C* **2016**, *120*, 21946−21954.

(19) Cao, Y.; Cong, S.; Cao, X.; Wu, F.; Liu, Q.; Amer, M. R.; Zhou, C. Review of electronics based on single-walled carbon nanotubes. *Top. Curr. Chem.* **2017**, *375*, 75.

(20) Kim, K. K.; Yoon, S. M.; Park, H. K.; Shin, H. J.; Kim, S. M.; Bae, J. J.; Cui, Y.; Kim, J. M.; Choi, J.-Y.; Lee, Y. H. Doping strategy of carbon nanotubes with redox chemistry. *New J. Chem.* **2010**, *34*, 2183−2188.

(21) Kim, K. K.; Kim, S. M.; Lee, Y. H. Chemically conjugated carbon nanotubes and graphene for carrier modulation. *Acc. Chem. Res.* **2016**, *49*, 390−399.

(22) Yu, W. J.; Lee, Y. H. Strategy for carrier control in carbon nanotube transistors. *ChemSusChem* **2011**, *4*, 890−904.

(23) Kim, S. M.; Jang, J. H.; Kim, K. K.; Park, H. K.; Bae, J. J.; Yu, W. J.; Lee, I. H.; Kim, G.; Loc, D. D.; Kim, U. J.; Lee, E. H.; Shin, H. J.; Choi, J. Y.; Lee, Y. H. Reduction-controlled viologen in bisolvent as an environmentally stable n-type dopant for carbon nanotubes. *J. Am. Chem. Soc.* **2009**, *131*, 327−331.

(24) Britz, D. A.; Khlobystov, A. N. Noncovalent interactions of molecules with single walled carbon nanotubes. *Chem. Soc. Rev.* **2006**, *35*, 637−659.

(25) Takenobu, T.; Takano, T.; Shiraishi, M.; Murakami, Y.; Ata, M.; Kataura, H.; Achiba, Y.; Iwasa, Y. Stable and controlled amphoteric doping by encapsulation of organic molecules inside carbon nanotubes. *Nat. Mater.* **2003**, *2*, 683−688.

(26) Lu, J.; Nagase, S.; Yu, D.; Ye, H.; Han, R.; Gao, Z.; Zhang, S.; Peng, L. Amphoteric and controllable doping of Carbon nanotubes by encapsulation of organic and organometallic molecules. *Phys. Rev. Lett.* **2004**, *93*, No. 116804.

(27) Kim, K. S.; Cota-Sanchez, G.; Kingston, C. T.; Imris, M.; Simard, B.; Soucy, G. Large-scale production of single-walled carbon nanotubes by induction thermal plasma. *J. Phys. D: Appl. Phys.* **2007**, *40*, 2375−2387.

(28) Ding, J.; Li, Z.; Lefebvre, J.; Cheng, F.; Dubey, G.; Zou, S.; Finnie, P.; Hrdina, A.; Scoles, L.; Lopinski, G. P.; Kingston, C. T.; Simard, B.; Malenfant, P. R. Enrichment of large-diameter semiconducting SWCNTs by polyfluorene extraction for high network density thin film transistors. *Nanoscale* **2014**, *6*, 2328−2339.

DOI: 10.1021/acsomega.8b00383
ACS Omega 2018, 3, 3413−3419

(29) Zheng, M.; Diner, B. A. Solution redox chemistry of carbon nanotubes. *J. Am. Chem. Soc.* **2004**, *126*, 15490−15494.
(30) Paillet, M.; Michel, T.; Zahab, A.; Nakabayashi, D.; Jourdain, V.; Parret, R.; Meyer, J.; Sauvajol, J. L. Probing the structure of single-walled carbon nanotubes by resonant Raman scattering. *Phys. Status Solidi B* **2010**, *247*, 2762−2767.
(31) Lee, A. J.; Wang, X.; Carlson, L. J.; Smyder, J. A.; Loesch, B.; Tu, X.; Zheng, M.; Krauss, T. D. Bright fluorescence from individual single-walled carbon nanotubes. *Nano Lett.* **2011**, *11*, 1636−1640.
(32) Kim, S. M.; Kim, K. K.; Duong, D. L.; Hirana, Y.; Tanaka, Y.; Niidome, Y.; Nakashima, N.; Kong, J.; Lee, Y. H. Spectroscopic determination of the electrochemical potentials of n-type doped carbon nanotubes. *J. Phys. Chem. C* **2012**, *116*, 5444−5449.
(33) Matsuda, K.; Miyauchi, Y.; Sakashita, T.; Kanemitsu, Y. Nonradiative exciton decay dynamics in hole-doped single-walled carbon nanotubes. *Phys. Rev. B* **2010**, *81*, No. 033409.
(34) Aguirre, C. M.; Levesque, P. L.; Paillet, M.; Lapointe, F.; St. Antoine, B. C.; Desjardins, P.; Martel, R. The role of the oxygen/water redox couple in suppressing electron conduction in field-effect transistors. *Adv. Mater.* **2009**, *21*, 3087−3091.
(35) Strano, M. S.; Huffman, C. B.; Moore, V. C.; O'Connell, M. J.; Haroz, E. H.; Hubbard, J.; Miller, M.; Rialon, K.; Kittrell, C.; Ramesh, S.; Hauge, R. H.; Smalley, R. E. Reversible, band-gap-selective protonation of single-walled carbon nanotubes in solution. *J. Phys. Chem. B* **2003**, *107*, 6979−6985.
(36) Duong, D. L.; Lee, S. M.; Lee, Y. H. Origin of unipolarity in carbon nanotube field effect transistors. *J. Mater. Chem.* **2012**, *22*, 1994−1997.
(37) Moonoosawmy, K. R.; Kruse, P. Cause and consequence of carbon nanotube doping in water and aqueous media. *J. Am. Chem. Soc.* **2010**, *132*, 1572−1577.
(38) Klinke, C.; Chen, J.; Afzali, A.; Avouris, P. Charge transfer induced polarity switching in carbon nanotube transistors. *Nano Lett.* **2005**, *5*, 555−558.
(39) Okano, M.; Nishihara, T.; Yamada, Y.; Kanemitsu, Y. Chemical doping-induced changes in optical properties of single-walled carbon nanotubes. *Jpn. J. Appl. Phys.* **2014**, *53*, No. 05FD02.
(40) O'Connell, M. J.; Eibergen, E. E.; Doorn, S. K. Chiral selectivity in the charge-transfer bleaching of single-walled carbon nanotube spectra. *Nat. Mater.* **2005**, *4*, 412−418.
(41) Hirana, Y.; Juhasz, G.; Miyauchi, Y.; Mouri, S.; Matsuda, K.; Nakashima, N. Empirical prediction of electronic potentials of single-walled carbon nanotubes with a specific chirality (n,m). *Sci. Rep.* **2013**, *3*, No. 2959.
(42) Han, J. Y.; Swarts, J. C.; Sykes, A. G. Kinetic studies on the hydrazine and phenylhydrazine reductions of the *Escherichia coli* R2 subunit of ribonucleotide reductase. *Inorg. Chem.* **1996**, *35*, 4629−4634.
(43) Pénicaud, A.; Poulin, P.; Derré, A.; Anglaret, E.; Petit, P. Spontaneous dissolution of a single-wall carbon nanotube salt. *J. Am. Chem. Soc.* **2005**, *127*, 8−9.
(44) Fogden, S.; Howard, C. A.; Heenan, R. K.; Skipper, N. T.; Shaffer, M. S. P. Scalable method for the reductive dissolution, purification, and separation of single-walled carbon nanotubes. *ACS Nano* **2012**, *6*, 54−62.
(45) Clancy, A. J.; Melbourne, J.; Shaffer, M. S. P. A one-step route to solubilised, purified or functionalised single-walled carbon nanotubes. *J. Mater. Chem. A* **2015**, *3*, 16708−16715.
(46) Ramesh, S.; Ericson, L. M.; Davis, V. A.; Saini, R. K.; Kittrell, C.; Pasquali, M.; Billups, W. E.; Adams, W. W.; Hauge, R. H.; Smalley, R. E. Dissolution of pristine single walled carbon nanotubes in superacids by direct protonation. *J. Phys. Chem. B* **2004**, *108*, 8794−8798.
(47) Zhou, J.; Maeda, Y.; Lu, J.; Tashiro, A.; Hasegawa, T.; Luo, G.; Wang, L.; Lai, L.; Akasaka, T.; Nagase, S.; Gao, Z.; Qin, R.; Mei, W. N.; Li, G.; Yu, D. Electronic-type and diameter-dependent reduction of single-walled carbon nanotubes induced by adsorption of electron-donor molecules. *Small* **2009**, *5*, 244−255.
(48) Lefebvre, J. Real time hyperspectroscopy for dynamical study of carbon nanotubes. *ACS Nano* **2016**, *10*, 9602−9607.
(49) Zhou, W.; Vavro, J.; Nemes, N. M.; Fischer, J. E.; Borondics, F.; Kamaras, K.; Tanner, D. Charge transfer and Fermi level shift in p-doped single-walled carbon nanotubes. *Phys. Rev. B* **2005**, *71*, No. 205423.
(50) Kim, S. N.; Luo, Z.; Papadimitrakopoulos, F. Diameter and metallicity dependent redox influences on the separation of single-wall carbon nanotubes. *Nano Lett.* **2005**, *5*, 2500−2504.
(51) Lu, J.; Lai, L.; Luo, G.; Zhou, J.; Qin, R.; Wang, D.; Wang, L.; Mei, W. N.; Li, G.; Gao, Z.; Nagase, S.; Maeda, Y.; Akasaka, T.; Yu, D. Why semiconducting single-walled carbon nanotubes are separated from their metallic counterparts. *Small* **2007**, *3*, 1566−1576.
(52) Nonoguchi, Y.; Ohashi, K.; Kanazawa, R.; Ashiba, K.; Hata, K.; Nakagawa, T.; Adachi, C.; Tanase, T.; Kawai, T. Systematic conversion of single walled carbon nanotubes into n-type thermoelectric materials by molecular dopants. *Sci. Rep.* **2013**, *3*, No. 3344.
(53) Kozinsky, B.; Marzari, N. Static dielectric properties of carbon nanotubes from First Principles. *Phys. Rev. Lett.* **2006**, *96*, No. 166801.
(54) Krupke, R.; Hennrich, F.; Löhneysen, H. V.; Kappes, M. M. Separation of metallic from semiconducting single-walled carbon nanotubes. *Science* **2003**, *301*, 344−347.
(55) Ding, J.; Li, Z.; Lefebvre, J.; Cheng, F.; Dunford, J. L.; Malenfant, P. R.; Humes, J.; Kroeger, J. A hybrid enrichment process combining conjugated polymer extraction and silica gel adsorption for high purity semiconducting single-walled carbon nanotubes (SWCNT). *Nanoscale* **2015**, *7*, 15741−15747.
(56) Shea, M. J.; Mehlenbacher, R. D.; Zanni, M. T.; Arnold, M. S. Experimental measurement of the binding configuration and coverage of chirality-sorting polyfluorenes on carbon nanotubes. *J. Phys. Chem. Lett.* **2014**, *5*, 3742−3749.
(57) Gerstel, P.; Klumpp, S.; Hennrich, F.; Poschlad, A.; Meded, V.; Blasco, E.; Wenzel, W.; Kappes, M. M.; Barner-Kowollik, C. Highly selective dispersion of single-walled carbon nanotubes via polymer wrapping: a combinatorial study via modular conjugation. *ACS Macro Lett.* **2014**, *3*, 10−15.
(58) Coleman, J. N.; Fleming, A.; Maier, S.; O'Flaherty, S.; Minett, A. I.; Ferreira, M. S.; Hutzler, S.; Blau, W. J. Binding kinetics and SWNT bundle dissociation in low concentration polymer-nanotube dispersions. *J. Phys. Chem. B* **2004**, *108*, 3446−3450.
(59) Deria, P.; Olivier, J.-H.; Park, J.; Therien, M. J. Potentiometric, electronic, and transient absorptive spectroscopic properties of oxidized single-walled carbon nanotubes helically wrapped by ionic, semiconducting polymers in aqueous and organic media. *J. Am. Chem. Soc.* **2014**, *136*, 14193−14199.
(60) Polo, E.; Kruss, S. Impact of redox-active molecules on the fluorescence of polymer-wrapped carbon nanotubes. *J. Phys. Chem. C* **2016**, *120*, 3061−3070.
(61) Fong, D.; Bodnaryk, W. J.; Rice, N. A.; Saem, S.; Moran-Mirabal, J. M.; Adronov, A. Influence of polymer electronics on selective dispersion of single-walled carbon nanotubes. *Chem. − Eur. J.* **2016**, *22*, 14560−14566.

DOI: 10.1021/acsomega.8b00383
ACS Omega 2018, 3, 3413−3419